ISSN (e): 2250 – 3005 || Volume, 14 || Issue, 4|| Jul. - Aug. – 2024 ||
International Journal of Computational Engineering Research (IJCER)

Modeling Diphtheria Pathogen Dynamics and Vaccine Strategies Considering Vaccine Hesitancy, Coverage, and Immunization Impact on Transmission

Eloho B. Akponana[1], Ngozika J. Egbune[2], Eirene O. Arierhie[3], Okedoye M. Akindele[4]

[1,2,3]*Doctoral Research Students,*
Department of Mathematics,
Federal University of Petroleum Resources, Effurun, Delta State, Nigeria.
[4] *Professor of Applied Mathematics,*
Department of Mathematics,
Federal University of Petroleum Resources, Effurun, Delta State, Nigeria.
Corresponding Author: Okedoye M. Akindele, okedoye.akindele@fupre.edu.ng

ABSTRACT
Infectious diseases such as diphtheria present ongoing global public health challenges, requiring robust prevention and control strategies. This abstract examines the transmission dynamics of diphtheria through a mathematical model that integrates pathogen behavior with vaccination strategies. The model incorporates compartments for susceptible individuals, infected cases, and vaccinated populations, considering factors like transmission rates, vaccination coverage, and waning immunity. A key focus is the impact of vaccine hesitancy, a significant factor affecting vaccination uptake. By incorporating vaccine hesitancy into the model, the study assesses its influence on disease spread and the effectiveness of immunization programs in controlling outbreaks. The findings emphasize the critical role of high vaccine coverage in reducing transmission and highlight the risk of disease resurgence due to insufficient vaccination or waning immunity. This research underscores the importance of sustained immunization efforts and informs public health strategies aimed at improving vaccine acceptance and coverage. By combining theoretical modelling with practical implications, the study provides valuable insights for policymakers and healthcare professionals committed to controlling diphtheria and similar infectious diseases, emphasizing the necessity of addressing vaccine hesitancy to achieve long-term public health goals.
KEYWORDS: *vaccine hesitancy, Vaccination impact, Waning immunity, Disease-free equilibrium, Control measures, Infection spread, Diphtheria Pathogen Dynamics and Vaccine Strategies.*
AMS Subject Classification: 92A10, 92B05

Date of Submission: 03-08-2024 Date of acceptance: 13-08-2024

I. INTRODUCTION

Infectious diseases remain a significant global health concern, with historical and ongoing threats posed by pathogens like Corynebacterium diphtheriae, the causative agent of diphtheria. Despite advancements in medical science and vaccination programs, diphtheria continues to pose challenges in both developed and developing countries. Understanding the dynamics of diphtheria transmission and optimizing vaccination strategies are crucial for effective disease control and prevention.

Diphtheria has a storied history as a major public health threat, particularly before the introduction of vaccines. The disease is characterized by a thick membrane formation in the throat and upper respiratory tract, often leading to severe complications such as airway obstruction and myocarditis. Before widespread immunization, diphtheria outbreaks were frequent and devastating, especially among children and adolescents [1]. The advent of diphtheria toxoid vaccines, first introduced in the 1920s and later combined into the DTP (diphtheria-tetanus-pertussis) vaccine, marked a turning point in disease prevention efforts. Vaccination programs have successfully reduced diphtheria incidence worldwide, contributing to its near-elimination in many developed countries. However, sporadic outbreaks and endemic transmission still occur, particularly in regions with suboptimal vaccination coverage and health infrastructure [2]. C. diphtheriae is primarily transmitted through

respiratory droplets from infected individuals or carriers. The bacterium colonizes the upper respiratory tract, where it produces diphtheria toxin—a potent exotoxin responsible for the disease's clinical manifestations. The dynamics of diphtheria transmission are influenced by various factors, including population density, socioeconomic conditions, and immunization coverage rates [3]. Mathematical modelling provides a valuable tool for understanding these transmission dynamics. Compartmental models, such as the susceptible-infected-recovered (SIR) framework adapted for diphtheria, divide populations into compartments based on disease status (susceptible, infected, recovered) and vaccination status. These models incorporate parameters such as transmission rates, vaccine efficacy, and the duration of immunity to simulate disease spread and evaluate intervention strategies [4].

Vaccination is the cornerstone of diphtheria control strategies, aimed at achieving herd immunity by reducing the susceptible population's size. The DTP vaccine, comprising diphtheria toxoid, tetanus toxoid, and acellular pertussis components, is routinely administered to infants and young children worldwide. Booster doses in adolescence and adulthood help maintain immunity levels and prevent outbreaks [5]. Despite vaccine availability, challenges persist in achieving and sustaining high immunization coverage. Vaccine hesitancy—a complex phenomenon influenced by factors such as misinformation, mistrust in healthcare authorities, and cultural beliefs—poses a significant barrier to achieving optimal vaccination rates. Addressing vaccine hesitancy requires targeted communication strategies, community engagement, and trust-building efforts [6].

The duration of vaccine-induced immunity against diphtheria is an essential consideration for immunization programs. While primary vaccination provides robust protection, immunity may wane over time, particularly in older adults and individuals without recent booster doses. Waning immunity increases susceptibility to infection and poses challenges for maintaining herd immunity levels within populations [7]. Mathematical models that incorporate waning immunity dynamics help predict the long-term effectiveness of vaccination programs and inform policy decisions regarding booster dose recommendations. These models assess the potential resurgence of diphtheria in populations with declining immunity levels and guide strategies for maintaining high vaccine coverage rates [8]. Despite the proven efficacy of diphtheria vaccines, vaccine hesitancy remains a significant challenge in achieving and maintaining high immunization coverage. Vaccine hesitancy is influenced by a complex interplay of factors including safety concerns, misinformation, religious beliefs, and distrust in healthcare systems [9]. These factors can undermine confidence in vaccination programs, leading to suboptimal vaccine uptake and reduced community immunity.

Recent studies highlight the detrimental effects of vaccine hesitancy on disease control efforts. For instance, outbreaks of vaccine-preventable diseases, including diphtheria, have been attributed to pockets of unvaccinated individuals within communities [10]. Inadequate vaccine coverage due to hesitancy increases the risk of disease resurgence, particularly in populations where vaccination rates fall below the threshold required for herd immunity [11]. Addressing vaccine hesitancy requires multifaceted strategies tailored to specific cultural and social contexts. Effective communication campaigns that provide accurate information about vaccines' safety, efficacy, and importance in disease prevention are essential [12]. Engaging with communities through trusted healthcare providers, community leaders, and educational initiatives can help build trust and address concerns related to vaccination [13].

Mathematical models play a crucial role in understanding the dynamics of diphtheria transmission and evaluating the impact of vaccination strategies. These models integrate biological parameters such as transmission rates, vaccine efficacy, and population demographics to simulate disease spread under different scenarios [14]. By quantifying the effectiveness of vaccination programs, models inform policy decisions on vaccination schedules, booster doses, and outbreak response strategies [15]. One notable model is the susceptible-infected-vaccinated-recovered (SIVR) framework, which extends traditional SIR models to include compartments for vaccinated individuals and those with waning immunity. This allows for a more nuanced analysis of vaccine coverage and its impact on disease transmission dynamics over time [16]. Models also assess the potential consequences of vaccine hesitancy by simulating scenarios with varying levels of vaccine uptake and community immunity.

Achieving high vaccine coverage is essential for diphtheria control, but it requires overcoming logistical challenges and addressing disparities in access to immunization services. In low-resource settings, limited infrastructure, vaccine supply chains, and healthcare worker capacity can hinder vaccination efforts [17]. Strengthening health systems, expanding immunization outreach programs, and integrating vaccination with primary healthcare services are critical strategies for improving vaccine coverage and equity [18]. Furthermore, ensuring vaccine affordability and accessibility is essential for global vaccination efforts. International partnerships, such as the Global Alliance for Vaccines and Immunization (GAVI), play a vital role in securing vaccine supplies and supporting immunization programs in resource-limited settings [19]. Sustainable financing mechanisms and advocacy for political commitment to immunization are necessary to maintain progress towards disease elimination goals.

Akponana et al. (2024) tackle the ongoing public health issue of diphtheria, which persists despite effective vaccines. They presented a mathematical model with five compartments: Susceptible (S), Infected (I), Vaccinated (V), Vaccine-Induced Immunity (W), and Recovered (R) to study the transmission dynamics of the disease. By analyzing key model properties such as the disease-free equilibrium and basic reproduction number, the study evaluated the conditions under which diphtheria may spread or be controlled. Numerical simulations were used to examine the effects of vaccination coverage, waning immunity, and susceptibility on disease transmission. Their findings suggest that combining vaccination, effective treatment, and contact tracing can significantly reduce and manage diphtheria outbreaks [20]. Arierhie et al. (2024) explored the critical role of immunization in public health, particularly underscored by the urgent need for COVID-19 vaccines during the pandemic. They employed a deterministic SEIVR model to analyze vaccine deployment strategies and their impact. Their research focused on understanding disease-free and endemic equilibria, calculating the basic reproduction number (R_0), and assessing stability through Jacobian matrix analysis. Their findings highlight a calculated (R_0) value of approximately 1.1251426e-10, indicating a very low potential for COVID-19 transmission. This suggests that vaccination efforts can significantly reduce the spread of the disease. Overall, the study emphasized the effectiveness of vaccines in creating immunity and preventing severe illness associated with COVID-19, thereby contributing valuable insights to ongoing global vaccination strategies [21].

Akponana et al. (2023) in their study addressed the persistent public health challenge posed by diphtheria through mathematical modelling. They develop a model to simulate the transmission dynamics of the disease, evaluating the impact of vaccination coverage, waning immunity, and susceptibility on its spread. Their findings underscore the effectiveness of combined strategies including vaccination, treatment, and contact tracing in controlling outbreaks. The research highlights the need for robust public health policies informed by mathematical models to mitigate the burden of diphtheria and identifies gaps in understanding, particularly concerning asymptomatic carriers, warranting further investigation [22]. Egbune et al. (2024) investigated the dynamics and control of diphtheria using mathematical modeling, focusing particularly on the effectiveness of Diphtheria Antitoxin (DAT) in mitigating the disease's impact. They developed compartmental models and formulated a system of differential equations to capture the complexities of diphtheria transmission. Utilizing numerical solutions such as the Runge-Kutta Fehlberg method, they analyzed the dynamics and assess the potential impact of DAT administration on disease outcomes. Their findings underscore the crucial role of DAT efficiency in reducing disease severity, preventing severe cases, and curbing epidemic spread. By exploring various scenarios and sensitivity analyses of model parameters, the study provides insights into optimal strategies for controlling and intervening in diphtheria outbreaks effectively. Overall, this research enhances understanding of diphtheria epidemiology and informs public health policies aimed at improving vaccination coverage and availability of DAT, thereby contributing to sustainable disease control and prevention efforts [23].

By synthesizing current knowledge and evidence from epidemiological studies, mathematical modelling, and public health interventions, this study seeks to assess the effectiveness of vaccination strategies in reducing diphtheria incidence and achieving herd immunity, with a focus on vaccine coverage and hesitancy and explore the impact of waning immunity on diphtheria epidemiology and the implications for vaccine policy and public health responses.

II. MODEL FORMULATION

The mathematical model for diphtheria transmission includes five compartments (S, I, V, W, R) representing different states of individuals related to the disease. It extends the basic epidemiological framework with parameters like recruitment rate (Λ), transition rate (β), and natural death rate (μ). Vaccination (ω) leads individuals to immunity or recovery, with potential immunity loss over time. This model analyzes diphtheria dynamics, vaccination impact, and compartmental interactions shown in the diagram below: The compartmental diagram for the mathematical model describing the interactions between the various compartments is shown in the figure below:

The dynamics of each compartment are described by a set of differential equations which are given below

$$\frac{dS}{dt} = \Lambda + n\xi W + \tau R - \frac{\beta SI}{N} - \mu S - \frac{\eta qSV}{N} \quad (1)$$

$$\frac{dI}{dt} = \frac{\beta SI}{N} + (1-n)\xi W - \eta \mathrm{I} - \gamma I - (\mu + \delta)\mathrm{I} \quad (2)$$

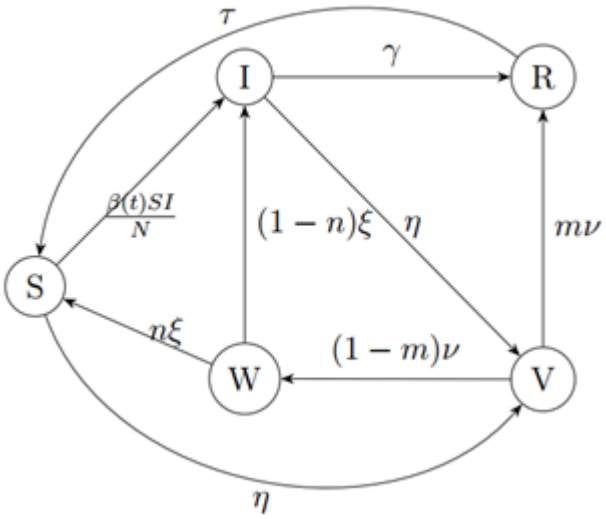

Figure 1: Compartmental Diagram

$$\frac{dV}{dt} = \frac{\eta qSV}{N} + \eta \mathrm{I} - \nu V - \mu V \quad (3)$$

$$\frac{dW}{dt} = (1-m)\nu V - \xi W - (\mu + \delta)W \quad (4)$$

$$\frac{dR}{dt} = \gamma I + m\nu V - (\tau + \mu)R \quad (5)$$

with

$S(0) = 990000, I(0) = 5000, V(0) = 3000, W(0) = 1000, R(0) = 1000, N(0) = 1000000$

Pathogen Dynamics:

- Incorporate a parameter (ω) representing pathogen dynamics, including factors such as pathogen evolution and persistence in the environment.
- The recovery rate (γ) in the equations is modified to reflect the impact of pathogen dynamics:

$$\gamma = \gamma 0(1 - \omega)$$

2. Vaccine Hesitancy:

- Introduce a parameter (ρ) representing the degree of vaccine hesitancy, which affects the uptake of vaccination.
- Modify the vaccination rate (η) in the equations to reflect the impact of vaccine hesitancy:

$$\eta = \eta_0 (1 - \rho)$$

3. Vaccine Coverage and Immunization:

Introduce a parameter ν representing rate of vaccination, then transmission rate is modified as

$$\beta = \beta 0(1 - \nu)$$

Introduce a parameter (C) representing vaccine coverage, which determines the proportion of the population eligible for vaccination. Introduce a parameter (ϕ) representing the effectiveness of immunization
campaigns in increasing vaccine coverage. Modify the vaccination rate (η) and immunization rate (ϕ) in the equations to reflect vaccine coverage and immunization efforts:

$$\eta = \eta_0 C(1 - \rho)$$

$$\phi = \phi_0 C$$

In these equations:
$S(t)$: Number of susceptible individuals at time *t*.
$I(t)$: Number of infectious individuals at time *t*.
$R(t)$: Number of recovered (or immune) individuals at time *t*.
$V(t)$: Number of vaccinated individuals at time *t*.

$W(t)$: Number of immunized individuals at time *t*.
N: Total population size.

ρ: Vaccine hesitancy.

ω: pathogen dynamics, including factors such as pathogen evolution and persistence in the environment
C: Vaccine coverage.

$n\xi$ proportion of individual whose immunity through vaccination waned and become infected

$(1-n)\xi$ proportion of individual whose immunity through vaccination waned and become infected

τ Recovered individual who became susceptible

ν Rate of vaccinated individuals transitioning from V to either W or R classes
Λ Recruitment into susceptible class
β Transmission rate
H Rate of infected individuals getting vaccinated
μ Natural death rate
δ Disease induced death rate
γ Recovery rate

q reduction in susceptibility due to vaccination

η vaccination rate

$\beta 0$: Baseline transmission rate.
$\gamma 0$: Baseline recovery rate.
$\rho 0$: Baseline vaccination rate.
$\phi 0$: Baseline immunization rate.

The total population is given by $N(t) = S(t) + I(t) + V(t) + W(t) + R(t)$ at any time t.

III. ANALYSIS OF THE MODEL

Qualitatively study the dynamical properties of the model (1) as follows:

3.1. Positivity and boundedness

For the model to be epidemiologically meaningful and mathematically well posed, it is necessary to establish that all solutions of system with positive initial data will remain positive for all times $t \geq 0$.

Positivity of Solution

Following from equations (2) to (5) we have

$$\frac{dI}{dt} \geq -(\eta + \gamma + \mu + \delta)I \Longrightarrow I(t) \geq I(0)e^{-(\eta+\gamma+\mu+\delta)t} \quad (6)$$

$$\frac{dV}{dt} \geq -(\nu + \mu)V \Longrightarrow V(t) \geq V(0)e^{-(\nu+\mu)t} \quad (7)$$

$$\frac{dW}{dt} \geq -(\xi + \mu + \delta)W \Longrightarrow W(t) \geq W(0)e^{-(\xi+\mu+\delta)t} \quad (8)$$

$$\frac{dR}{dt} \geq -(\tau + \mu)R \Longrightarrow R(t) \geq R(0)e^{-(\tau+\mu)t} \quad (9)$$

From equation (1),

$$\frac{dS}{dt} \geq -\left(\frac{\beta I}{N} + \mu + \frac{\eta q V}{N}\right)S \Rightarrow \frac{dS}{S} \geq -\left(\frac{\beta I}{N} + \mu + \frac{\eta q V}{N}\right)dt$$

which leads to

$$\frac{dS}{S} \geq -\left(\frac{\beta}{N}I(0)e^{-(\eta+\gamma+\mu+\delta)t} + \mu + \frac{\eta q}{N}V(0)e^{-(\nu+\mu)t}\right)dt$$

$$S(t) \geq \frac{\eta q V(0)}{N(\eta+\mu)}\left(e^{-(\nu+\mu)t} - 1\right) + \frac{\beta I(0)}{N(\eta + \gamma + \mu + \delta)}\left(e^{-(\eta+\gamma+\mu+\delta)t} - 1\right) - \mu t + S(0) \quad (10)$$

From equations (6) – (10) we can see that each equation in the system ensures positive derivatives for positive initial conditions. Thus, solutions $S(t), I(t), V(t), W(t), R(t)$ remain positive for all times $t \geq 0$, which proves the positivity of solutions.

Boundedness

To ensure the solutions to the given system of differential equations are bounded, we need to demonstrate that each variable remains within finite limits for all time. This is essential for the solutions to be both non-negative and meaningful in the context of the model's application.

To prove the boundedness, we will show that the total population

$$N(t) = S(t) + I(t) + V(t) + W(t) + R(t)$$

is bounded.

Therefore, adding all the equations of the system together, gives

$$\frac{dN}{dt} = \frac{dS}{dt} + \frac{dI}{dt} + \frac{dV}{dt} + \frac{dW}{dt} + \frac{dR}{dt}$$

$$= \left(\Lambda + n\xi W + \tau R - \frac{\beta SI}{N} - \mu S - \frac{\eta qSV}{N}\right) + \left(\frac{\beta SI}{N} + (1-n)\xi W - \eta \mathrm{I} - \gamma I - (\mu + \delta)\mathrm{I}\right)$$

$$+ \left(\frac{\eta qSV}{N} + \eta \mathrm{I} - \nu V - \mu V\right) + \left((1-m)\nu V - \xi W - (\mu + \delta)W\right) + (\gamma I + m\nu V - (\tau + \mu)R)$$

$$\frac{dN}{dt} = \Lambda - \mu S - (\mu + \delta)\mathrm{I} - \mu V - (\mu + \delta)W - \mu R$$

$$\frac{dN}{dt} = \Lambda - \mu(S + \mathrm{I} + \mathrm{V} + \mathrm{W} + \mathrm{R}) - \delta \mathrm{I} - \delta W$$

The recruitment rate Λ and death terms suggest that the population is affected by a constant inflow and various outflows. As N increases, the term $-\mu N$ becomes dominant, indicating that $\frac{dN}{dt} < 0$ for sufficiently large N, thereby limiting population growth. Thus, $N(t)$ is bounded above by:

$$N(t) \leq \frac{\Lambda}{\mu}$$

for large t. This ensures that N remains finite and provides a bound based on the parameters Λ and μ.

3.2. Equilibrium Points

Identifying equilibrium points in disease mathematical models is essential for effective decision-making regarding disease control and eradication strategies. In infectious disease modeling, the Disease-Free Equilibrium (DFE) point and the Disease-Endemic Equilibrium (DEE) point are of particular importance. Analyzing these points offers significant insights into disease dynamics and management.

3.2.1. The Disease-Free Equilibrium (DFE)

In mathematical models of infectious diseases, the Disease-Free Equilibrium (DFE) is a state where no infections occur in the population. This stable point indicates the disease is not spreading. In epidemiology and disease control, understanding the DFE is essential for evaluating the success of interventions designed to prevent or eradicate infectious diseases. Here we take $I = 0$, which when solved results in two cases namely; when $S = \frac{N(\mu+\nu)}{\eta q}$ or $\mathrm{V} = 0$

For case 1, when $\mathrm{V} = 0$*, we get our DFE to be*

$$S = \frac{\Lambda}{\mu}, \mathrm{V} = \mathrm{W} = \mathrm{R} = 0$$

Hence

$$DFE_1 = (S, I, V, W, R) = \left(\frac{\Lambda}{\mu}, 0, 0, 0, 0\right) \quad (11)$$

For case 2, when $S = \frac{N(\mu+\nu)}{\eta q}$, we get our DFE to be

$$S = \frac{N(\mu+\nu)}{\eta q}, \mathrm{V} = \mathrm{W} = \mathrm{R} = 0 \text{ where } \mathrm{q} = \frac{\mu N(\mu+\nu)}{\Lambda\eta}$$

Hence

$$DFE_2 = (S, I, V, W, R) = \left(\frac{N(\mu+\nu)}{\eta q}, 0, 0, 0, 0\right) \tag{12}$$

3.2.2. The Disease-Endemic Equilibrium (DEE)

In mathematical models of infectious diseases, the Endemic Equilibrium Point (EEP) represents a stable state where the disease persists at a steady level within a population over time. The EEP describes a situation where the disease continues to spread but remains stable due to balanced transmission and recovery rates. Understanding the EEP is crucial for assessing long-term disease control strategies and predicting the impact of interventions on disease prevalence. We then solve the entire system of equations to get

$$S_e = \frac{1}{2}\frac{Nc_2c_8 + \beta c_3 \pm \sqrt{N^2{c_2}^2{c_8}^2 - 2N\beta(c_2c_8 - 2c_7)c_2 + \beta^2{c_3}^2}}{\beta c_2}$$

$$I_e = \frac{\begin{pmatrix}((N\mu c_8 - \Lambda\beta)(Nc_8 - \beta c_6)(Nc_8c_9 - \beta c_5){c_2}^2 - 2\beta c_7 N\left(\left(\left(-\frac{1}{2}c_6\mu - \frac{1}{2}\Lambda\right)c_9 - \frac{1}{2}c_5\mu\right)\beta\right.\\ \left.+Nc_8c_9\mu\right)c_2 - \beta^2 N\mu c_9c_7c_3)\sqrt{N^2{c_2}^2{c_8}^2 - 2N\beta(c_2c_8 + 2c_7)c_2 + \beta^2{c_3}^2} - Nc_8(N\mu c_8\\ -\Lambda\beta)(Nc_8 - \beta c_6)(Nc_8c_9 - \beta c_5){c_2}^3 + \beta(-\beta^3\Lambda c_6c_5c_3 + (c_6\Lambda c_9 + c_5(\mu c_6 + \Lambda))(c_3c_8\\ +2c_7)N\beta^2 - (c_3c_8 + 3c_7)((\mu c_6 + \Lambda)c_9 + c_5\mu)c_8N^2\beta + N^3{c_8}^2c_9\mu(c_3c_8 + 4c_7)){c_2}^2\\ +\beta^2c_7N(-((\mu c_6 + \Lambda)c_9 + c_5\mu)c_3\beta + Nc_9\mu(c_3c_8 - 2c_7))c_2 + N\beta^3\mu{c_2}^3c_7c_9)\end{pmatrix}}{\begin{pmatrix}\beta\left(\left((c_6(-c_5c_8 + c_4)\beta^2 - ((-c_6c_9 - c_5)c_8 + c_6q\eta\tau\gamma + c_5\eta + c_4)c_8N\beta - {c_8}^2N^2(c_8c_9\right.\right.\\ \left.-\eta\left(\gamma q\tau + c_9\right)\right)\left){c_2}^2 + 2\beta\left(-\frac{1}{2}(c_7 + c_1)(c_6c_9 + c_5)\beta + \left(c_9\left(c_7 + \frac{1}{2}c_1\right)c_8 - \frac{1}{2}c_7\eta(\gamma q\tau\right.\right.\\ \left.+c_9)\right)N\right)c_2 + c_3c_9\beta^2(c_7 + c_1)\sqrt{N^2{c_2}^2{c_8}^2 - 2N\beta(c_2c_8 + 2c_7)c_2 + \beta^2{c_3}^2} + Nc_8(-c_6\\ (-c_5c_8 + c_4)\beta^2 + ((-c_6c_9 - c_5)c_8 + c_6q\eta\tau\gamma + c_5\eta + c_4)c_8N\beta + {c_8}^2N^2(c_8c_9 - \eta(\gamma q\tau\\ +c_9)){c_3}^2 - \beta(-c_6(-c_3c_5c_8 - 2c_1c_5 + c_3c_4 - 2c_5c_7)\beta^2 + (-c_3(c_6c_9 + c_5){c_8}^2 + (-3(c_7\\ +\frac{1}{3}c_1)c_6c_9 - 3c_5c_7 + c_3c_6q\eta\tau\gamma + (\eta c_5 + c_4)c_3 - c_5c_1)c_8 + 2c_7(\eta\gamma q\tau c_6 + \eta c_5 + c_4))\\ N\beta + (c_3{c_8}^2c_9 + ((-\eta c_3 + c_1 + 4c_7)c_9 - c_3q\eta\tau\gamma)c_8 - 3c_7\eta(\gamma q\tau + c_9))c_8N^2){c_2}^2 - \beta^2\\ (-c_3(c_7 + c_1)(c_6c_9 + c_5)\beta + c_7(c_3c_8c_9 + (-\eta c_3 - 2c_1 - 2c_7)c_9 - c_3q\eta\tau\gamma)N)c_2 - {c_3}^2\\ c_9\beta^3(c_7 + c_1)))\end{pmatrix}}$$

$$V_e = \frac{\eta I_e N}{-\eta q S_e + N\mu + N\nu}, \qquad W_e = \frac{(1-m)\nu\eta I_e N}{(-\eta q S_e + N\mu + N\nu)}$$

$$R_e = \frac{-I_e q\eta\gamma S_e + I_e N((\mu+\nu)\gamma + m\nu\eta)}{(-\eta q S_e + N\mu + N\nu)(\tau+\mu)}$$

where $c_1 = n\xi(1-m)\nu\eta N, c_2 = \eta q(\xi + \mu + \delta), c_3 = (N\mu + N\nu)(\xi + \mu + \delta),$ $c_4 = (N\gamma\tau(\mu+\nu) + m\tau\nu\eta N), c_5 = N(\tau+\mu)(\mu+\nu), c_6 = \frac{N\mu+N\nu}{\eta q}, c_7 = (1-n)\xi(1-m)\nu\eta N, c_8 = \left(\eta + \gamma + (\mu+\delta)\right), c_9 = \eta(\tau + \mu)q$

3.3. Stability Analysis

In epidemiological modeling, stability analysis is crucial for understanding the long-term behavior of disease dynamics within a population. For the *SIVWR* (Susceptible-Infectious-Vaccinated-Immunized-Recovered)

model, stability analysis helps determine whether the disease will eventually be eradicated or persist over time by examining the equilibrium solutions of the system.

At the Disease-Free Equilibrium (DFE), the Jacobian matrix of the system is computed and then evaluated at the DFE to assess its stability.

$$J|_{(S_0,I_0,V_0,W_0,R_0)} = \begin{bmatrix} -h_1-\lambda & -e_1 & -f_1 & n\xi & \tau \\ 0 & -g_1-\lambda & 0 & j_1 & 0 \\ 0 & \eta & -h_1-\lambda & 0 & 0 \\ 0 & 0 & -i_1 & -c_1-\lambda & 0 \\ 0 & \gamma & m\nu & 0 & -d_1-\lambda \end{bmatrix}$$

where

$$c_1 = (\xi+\mu+\delta), d_1 = (\tau+\mu),\ e_1 = \frac{\beta\Lambda}{\mu N},\ f_1 = \frac{\eta q\Lambda}{\mu N}, g_1 = (\eta+\ \gamma+\mu+\delta) - \frac{\beta\Lambda}{\mu N},$$
$$h_1 = (\nu+\mu) - \frac{\eta q\Lambda}{\mu N}, i_1 = (1-m)\nu, j_1 = (1-n)\xi$$

The characteristic polynomial is given by

$$32\lambda^5 + (16\mu + 16g_1 - 16h_1 + 16c_1 + 16\ d_1)\lambda^4 + (7\ d_1c_1 - 7\ d_1h_1 + 7\ d_1g_1 + 7\ d_1\mu$$
$$+8g_1\mu + 8c_1h_1 + 8c_1g_1 + 8c_1\mu - 8h_1g_1 - 8h_1\mu +\ d_1(\mu + c_1 + g_1 - h_1))\lambda^3 + (4i_1\eta j_1$$
$$-4c_1g_1h_1 + d_1(\mu c_1 + \mu g_1 - \mu h_1 + c_1g_1 - c_1h_1 - g_1h_1) + 3\mu c_1d_1 + 4\mu c_1g_1 - 4\mu c_1h_1$$
$$+3\mu\ d_1g_1 - 3\mu\ d_1h_1 - 4\mu\ g_1h_1 + 3c_1d_1h_1 - 3d_1g_1h_1)\lambda^2 + (2\eta\mu i_1j_1 + \eta d_1i_1j_1 + \mu c_1d_1g_1$$
$$-\mu c_1d_1h_1 - 2\mu c_1g_1h_1 - \mu d_1g_1h_1 - c_1d_1g_1h_1 + d_1(\eta i_1j_1 + \mu c_1g_1 - \mu c_1h_1 - c_1g_1h_1))\lambda$$
$$+d_1(\eta\mu i_1j_1 - \mu c_1g_1h_1)$$

The above characteristic polynomial equation is of the form

$$P(\lambda) = a_5\lambda^5 + a_4\lambda^4 + a_3\lambda^3 + a_2\lambda^2 + a_1\lambda + a_0 = 0$$

$a_5 = 32,$

$a_4 = 16\mu + 16g_1 - 16h_1 + 16c_1 + 16\ d_1,$

$a_3 = 7\ d_1c_1 - 7\ d_1h_1 + 7\ d_1g_1 + 7\ d_1\mu + 8g_1\mu + 8c_1h_1 + 8c_1g_1 + 8c_1\mu - 8h_1g_1 - 8h_1\mu$
$+\ d_1(\mu + c_1 + g_1 - h_1),$

$a_2 = 4i_1\eta j_1 - 4c_1g_1h_1 + d_1(\mu c_1 + \mu g_1 - \mu h_1 + c_1g_1 - c_1h_1 - g_1h_1) + 3\mu c_1d_1 + 4\mu c_1g_1 - 4\mu c_1h_1$
$+ 3\mu\ d_1g_1 - 3\mu\ d_1h_1 - 4\mu\ g_1h_1 + 3c_1d_1h_1 - 3d_1g_1h_1,$

$a_1 = 2\eta\mu i_1j_1 + \eta d_1i_1j_1 + \mu c_1d_1g_1 - \mu c_1d_1h_1 - 2\mu c_1g_1h_1 - \mu d_1g_1h_1 - c_1d_1g_1h_1$
$+ d_1(\eta i_1j_1 + \mu c_1g_1 - \mu c_1h_1 - c_1g_1h_1)$

$a_0 = d_1(\eta\mu i_1j_1 - \mu c_1g_1h_1)$

By Routh-Hurwitz criterion governing the polynomials of order 5 the system is stable if all and only if all roots of the equation have negative real parts. And for the system to be stable, all entries in the first column of the Routh array must be. From the Routh array construction we have 32 which is positive while for the rest to satisfy that condition

1. $a_4 > 0$
2. $b_{31} > 0$
3. $b_{41} > 0$
4. $b_{51} > a_3$

where $b_{31} = \frac{a_4a_3 - 32a_2}{a_4}, b_{41} = \frac{b_{31}a_2 - a_4b_{32}}{b_{31}}, b_{51} = \frac{b_{41}\,b_{32} - b_{31}b_{42}}{b_{41}}, b_{32} = \frac{a_4a_1 - 32a_0}{a_4}, b_{42} = \frac{b_{31}a_0}{b_{31}}$

From the expansion above, all the conditions are satisfied. Therefore, the disease-free equilibrium is locally asymptotically stable. This completes the proof.

3.4. The Basic Reproduction Number

The basic reproduction number, R_0, is the average number of secondary cases produced by one infected person in a fully susceptible population during their infective period. To find R_0, the next-generation matrix approach is employed. Let $X(t) = (I, V, W)$ and obtain that

$$X'(t) = \mathcal{F}(t) - \mathcal{V}(t)$$

where:

$$\mathcal{F}(t) = \begin{pmatrix} \frac{\beta S}{N} & 0 & (1-n)\xi \\ 0 & 0 & 0 \\ 0 & 0 & 0 \end{pmatrix}, \mathcal{V}(t) = \begin{pmatrix} -(\eta+\gamma+\mu+\delta) & 0 & 0 \\ \eta & \frac{\eta q S}{N} - (\nu+\mu) & 0 \\ 0 & (1-m)\nu & -(\xi+\mu+\delta) \end{pmatrix}$$

Evaluating the derivatives of F and V at the disease-free equilibrium point obtained above, yields $F\mathcal{V}^{-1}$ as seen below:

$$F\mathcal{V}^{-1} = \begin{pmatrix} \frac{(-\nu\xi(1-n)(1-m)N^2 + c_1 S^2 q\beta)\eta - N\beta S b_1 c_1}{N a_1(-S\eta q + N b_1)c_1} & -\frac{(1-n)\xi(1-m)\nu N}{(-S\eta q + N b_1)c_1} & -\frac{(1-n)\xi}{c_1} \\ 0 & 0 & 0 \\ 0 & 0 & 0 \end{pmatrix}$$

where $a_1 = (\eta+\gamma+\mu+\delta), b_1 = (\nu+\mu), c_1 = (\xi+\mu+\delta)$

By solving the dominant eigenvalue of the next generation matrix $F\mathcal{V}^{-1}$, we get the basic reproduction number to be

$$R_0 = -\frac{(-\nu\xi(1-n)(1-m)N^2 + c_1 S^2 q\beta)\eta - N\beta S b_1 c_1}{N a_1(-S\eta q + N b_1)c_1}$$

Therefore, the basic reproduction number of the given system of equations denoted by R_0 is:

$$R_0 = -\frac{(-N^2\nu\xi(1-n)(1-m)\mu^2 + \Lambda^2 c_1 q\beta)\eta - \Lambda N\beta\mu b_1 c_1}{N\mu a_1(-\Lambda\eta q + N\mu b_1)c_1}$$

3.5. Parameter Effects on the BRN

Sensitivity analysis helps determine the sensitivity index, measuring the relative change in a state variable with a change in a parameter. Using the approach by [24], we calculate the sensitivity indices of R_0 for model parameters, showing each parameter's role in disease transmission dynamics and prevalence. The sensitivity of a parameter, such as β, on R_0 is defined as:

$$\xi_\beta^{R_0} = \frac{\partial R_0}{\partial \beta} \times \frac{\beta}{R_0} \tag{13}$$

Consequently, the table below displays the sensitivity indices of the parameters affecting the Basic Reproduction Number.

Table: Sensitivity analysis on Basic Reproduction Number R_0

Parameter	Sensitivity Index	Parameter	Sensitivity Index
Λ	0.001135	ν	0.130283
β	0.001131	q	0.0000043
δ	-0.319836	η	0.914128
γ	-0.847458	ξ	0.443942
μ	-0.323325		

IV. DISCUSSION OF RESULTS

In this section, we present the results of our numerical simulation analysis for the SIVWR (Susceptible-Infectious-Vaccinated-Immunized-Recovered) model. This analysis is fundamental for understanding the long-term behavior of Diphtheria transmission within the population.

Figure 2 demonstrates the impact of the natural death rate (μ) on the infectious population. When $\mu = 0$, the infectious population declines slowly, indicating a prolonged infectious period that allows the disease to persist longer and complicates outbreak control. As μ increases (from 0.2 to 0.6), the decline in the infectious population becomes more rapid, reflecting a shorter duration of infectiousness and faster disease prevalence reduction. Higher natural death rates lead to quicker stabilization of the infectious population, suggesting that similar effects can be achieved through interventions like medical treatments and vaccination efforts. Figure 3 illustrates the effect of μ on the vaccinated population ($V(t)$) over 30 months. All curves show a decline in the vaccinated population, but

the rate varies with μ. The red curve ($\mu = 0$) shows the slowest decrease, with the vaccinated population remaining relatively stable. In contrast, as \(\mu\) increases, the decline becomes steeper: the black dashed curve ($\mu = 0.2$) shows a moderate decline, while the purple dash-dotted ($\mu = 0.4$) and blue dotted ($\mu = 0.6$) curves show increasingly rapid declines. This indicates that higher natural death rates significantly impact the vaccinated population, highlighting the need for continued vaccination efforts and minimized mortality to sustain effective immunity levels. Figure 4 shows the impact of the natural death rate (μ) on the immunized population ($W(t)$) over 30 months. With $\mu = 0$ (red curve), the immunized population steadily grows as individuals move into this class through vaccination or recovery, enhancing overall immunity. However, as μ increases (black dashed for $\mu = 0.2$, purple dash-dotted for $\mu = 0.4$, and blue dotted for $\mu = 0.6$), the immunized population declines more sharply. Higher mortality rates significantly reduce the number of immunized individuals, with the blue dotted curve showing the steepest decline, indicating that a high natural death rate quickly depletes the immunized class.

Figure 5 illustrates the effect of the recovery rate (γ) on the infected population ($I(t)$) over 30 months. Higher recovery rates lead to a significant reduction in the infected population. The red curve ($\gamma = 0$) represents a scenario with no recovery, resulting in unchecked growth of infections and potential severe outbreaks. As γ increases, the decline in the infected population becomes more pronounced: the black dashed curve ($\gamma = 0.2$) shows a moderate decrease, while the purple dash-dotted ($\gamma = 0.4$) and blue dotted ($\gamma = 0.6$) curves show increasingly rapid declines. This highlights the critical role of recovery in controlling disease spread and underscores the importance of enhancing recovery rates through effective treatments and healthcare interventions. Figure 6 shows the effect of different recovery rates (γ) on the recovered population ($R(t)$) over 30 months. The recovery rate (γ) indicates how quickly infected individuals recover and move into the recovered class. At $\gamma = 0$ (red curve), there is no recovery, so the recovered population remains low, indicating prolonged transmission and potential re-infections. As γ increases to 0.2 (black dashed curve), the recovered population rises sharply before gradually declining, reflecting the buildup of immunity and a subsequent decrease in new infections. Higher recovery rates γ=0.4 and γ=0.6, purple dash-dotted and blue dotted curves, respectively) lead to a rapid increase in the recovered population, peaking earlier and at higher levels. This quick recovery results in a substantial buildup of immunity, followed by a decline as the epidemic subsides. Figure 7 depicts the effect of varying vaccination rates (η) on the infected population ($I(t)$) over 30 months. The vaccination rate (η) indicates the speed at which infected individuals receive vaccines, reducing the number of active cases. This transition to the vaccinated class is vital for controlling disease spread. When $\eta = 0$ (red curve), the infected population declines slowly, as natural recovery and death are the main factors reducing infections. As the vaccination rate increases to $\eta = 0.2$ (black dashed curve), the decline in the infected population becomes steeper, showing that vaccination accelerates the decrease in infections. Higher vaccination rates $\eta = 0.4$ and $\eta = 0.6$, purple dash-dotted and blue dotted curves) result in an even faster decline, indicating that increased vaccination effectively curtails disease spread and mitigates the epidemic. Figure 8 shows the effect of varying vaccination rates (η) on the vaccinated population ($V(t)$)over 30 months. The vaccination rate (η) reflects how quickly infected individuals are vaccinated, crucial for reducing infection spread and building population immunity. With $\eta = 0$ (red curve), the vaccinated population remains nearly constant, relying only on natural immunity from recovery. As η increases to 0.2 (black dashed curve), the vaccinated population grows, enhancing immunity and reducing transmission. Higher rates $\eta = 0.4$ and $\eta = 0.6$, purple dash-dotted and blue dotted curves) show rapid expansion in the vaccinated population, indicating the effectiveness of vaccination in achieving herd immunity and reducing disease spread.

Figure 9 illustrates the impact of varying waning immunity rates (ξ) on the immunized population over 30 months. Without waning immunity ($\xi = 0$), the immunized population grows steadily, indicating lasting herd immunity. As ξ increases to 0.2, 0.4, and 0.6, the immunized population declines more rapidly, highlighting the need for ongoing vaccination efforts and booster doses to maintain protection and prevent outbreaks. Managing waning immunity is crucial for sustained community protection against diseases like diphtheria. The rate ν, which dictates how quickly vaccinated individuals transition from the V (vaccinated) class to either the W (immunized) or R (recovered) class as shown in Figure 10 and Figure 11, plays a crucial role in shaping the dynamics of these populations. When ν is high, individuals move rapidly from V to W or R This results in a swift reduction in the number of people in the vaccinated class, V, while potentially leading to a significant increase in the immunized class, W. However, if a large proportion of these individuals transitions to R (recovered), the growth in W might

be less pronounced, as fewer individuals are available to join the immunized group. With a moderate ν, the transition rates are balanced, which results in a steady but manageable decrease in the vaccinated class and a more controlled and gradual increase in the immunized class. This balance allows for a more stable buildup of immunity over time and can help maintain effective vaccination coverage. In contrast, a low ν indicates that individuals remain in the vaccinated class for a longer period before transitioning to W or R. This leads to a larger and more persistent V population, as fewer individuals are moving out of this class. Consequently, the growth of the immunized class W is slower, which can impact the overall effectiveness of the vaccination program. Slower transitions might delay the establishment of robust immunity within the population, potentially reducing the program's ability to achieve and maintain high levels of protection against disease outbreaks.

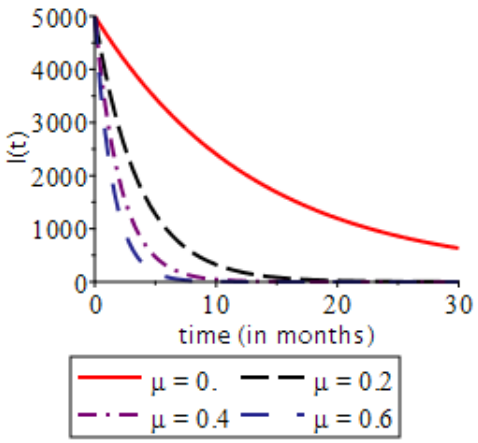

Figure 2: Effect of the natural mortality rate on the infected class.

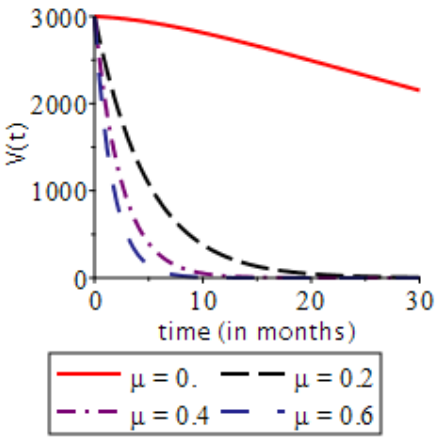

Figure 3: Effect of the natural mortality rate on the vaccinated class.

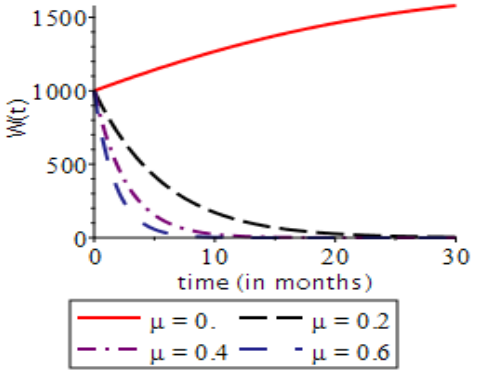

Figure 4: Effect of natural mortality rate on the immunized class.

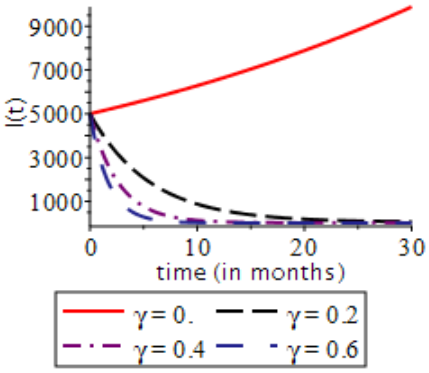

Figure 5: Effect of recovery rate on infected class.

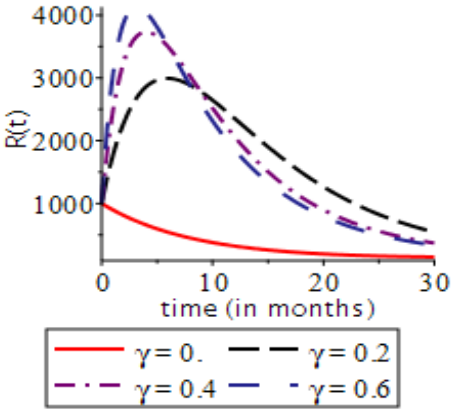

Figure 6: Effect of recovery rate on infected class.

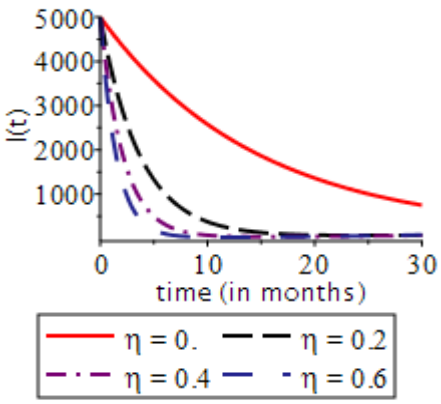

Figure 7: Effect of infected individuals getting vaccinated on the infected population.

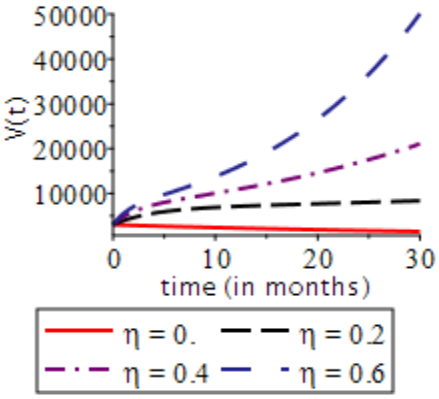

Figure 8: Effect of infected individuals getting vaccinated on the vaccinated population.

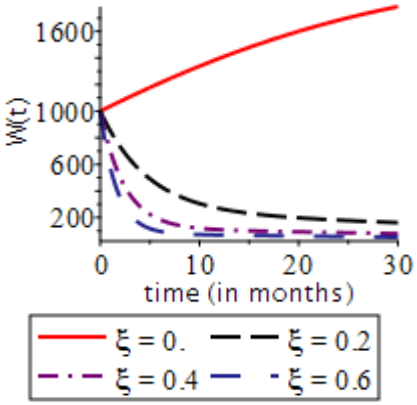

Figure 9: Effect of the waning immunity on the immunized population.

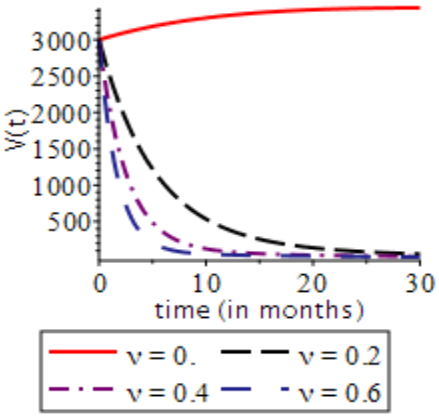

Figure 10: Effect of the natural mortality rate on the vaccinated population.

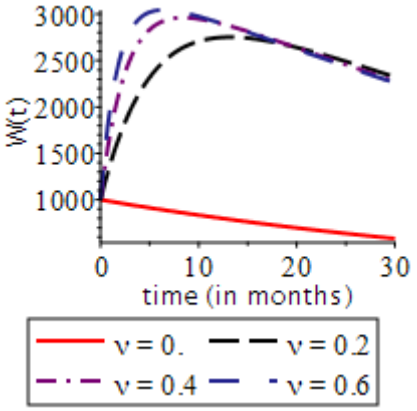

Figure 11: Effect of the natural mortality rate on the infected population.

4.2 Validation of Results

In the study by Akponana et al. (2024), the authors consider individuals with waning immunity to transition back into the susceptible population. However, in the current study, we posit a more nuanced approach, suggesting that individuals with waning immunity, despite being previously vaccinated, may not simply revert to a fully susceptible state. Instead, these individuals may experience re-infection by *Corynebacterium

diphtheriae*, although not necessarily with the same intensity as a primary infection. Moreover, those who have recovered from the disease might also become susceptible again if strict immunization protocols are not followed. This perspective suggests that the scenarios explored by Akponana et al. (2024) and Egbune et al. (2024) are specific instances within a broader framework presented in our current study. Our findings align with previous research when the additional assumptions about waning immunity and recovered individuals are accounted for, demonstrating that the results of our study extend and refine the understanding of diphtheria transmission dynamics as modeled in earlier works.

V. CONCLUSION

The analysis of diphtheria dynamics through the SIVWR model highlights the intricate relationship between vaccination strategies, natural death rates, recovery rates, and immunity waning. Higher natural death rates lead to quicker declines in the infectious and immunized populations, while increased recovery rates help manage disease spread and build immunity. Effective vaccination strategies, including higher vaccination rates and timely booster doses, are essential for reducing infections and maintaining herd immunity. Waning immunity poses a challenge to long-term vaccine effectiveness, underscoring the need for continued research and improved vaccine formulations. The numerical simulations of the SIVWR model reveal critical insights into how various parameters impact the dynamics of diphtheria transmission and vaccination strategies. The natural death rate (μ) significantly affects both the infectious and immunized populations. A higher μ leads to a quicker reduction in the infectious population, reflecting a shorter infectious period and faster disease stabilization. Conversely, it also accelerates the decline in the vaccinated and immunized populations, underscoring the sensitivity of these groups to mortality rates and highlighting the importance of maintaining vaccination efforts to ensure sustained immunity. The recovery rate (γ) plays a crucial role in managing disease spread. Higher recovery rates lead to a more rapid reduction in the infected population and an increase in the recovered class, which helps in building immunity and controlling the outbreak more effectively. This underscores the necessity of effective treatments and healthcare interventions to enhance recovery rates and manage disease transmission. The vaccination rates have a profound impact on controlling diphtheria as increased vaccination rates among infected individuals and the general population lead to a more significant and immediate reduction in infections and a faster expansion of the vaccinated population. This highlights the effectiveness of vaccination in reducing disease prevalence and the importance of higher vaccination coverage to achieve herd immunity. Waning immunity (ξ) affects the longevity of protection offered by vaccines. Without waning immunity, the immunized population grows steadily, indicating strong and lasting herd immunity. However, as waning immunity rates increase, the number of immunized individuals declines more rapidly, emphasizing the need for booster doses and improved vaccine formulations to maintain high levels of protection. The rate of transition from vaccinated to immunized or recovered classes (ν) also impacts vaccine effectiveness. High ν results in a rapid reduction of the vaccinated class but can boost the immunized population. In contrast, low ν leads to a larger and more persistent vaccinated class but slows the growth of the immunized class, which may affect overall vaccine program effectiveness.

From the discussion of result of this study, the following key finding are deduced:

- The SIVWR model highlights the critical roles of vaccination strategies, natural death rates, and recovery rates in managing diphtheria transmission and immunity.
- Higher natural death rates accelerate the decline of both infectious and immunized populations, impacting disease stabilization and long-term immunity.
- Increased recovery rates are essential for reducing infection spread and building immunity, emphasizing the need for effective treatments.
- Effective vaccination, including higher coverage and timely booster doses, is key to reducing infections and achieving herd immunity.
- Waning immunity challenges long-term vaccine effectiveness, necessitating booster doses and improved vaccine formulations.
- The transition rate from vaccinated to immunized classes influences overall vaccine program effectiveness, with higher rates boosting the immunized population.

REFERENCES

[1]. World Health Organization. (2020). Diphtheria vaccine: WHO position paper. Retrieved from [https://www.who.int/immunization/policy/position\papers/diphtheria/en/](https://www.who.int/immunization/policy/position_papers/diphtheria/en/)

[2]. Centers for Disease Control and Prevention. (2020). Diphtheria: Epidemiology and prevention of vaccine-preventable diseases. Retrieved from [https://www.cdc.gov/vaccines/pubs/pinkbook/dip.html]

[3]. Wagner, K. S., White, J. M., Neal, S., Crowcroft, N. S., & Kuprevičiene, N. (2016). Diphtheria in the postepidemic period, Europe, 2000-2009. Emerging Infectious Diseases, 22(12), 2186-2192.

[4]. Earn, D. J., & Rohani, P. (2004). The impact of vaccine efficacy and the resurgence of pertussis. American Journal of Epidemiology, 160(5), 457-465.
[5]. Plotkin, S. A., Orenstein, W. A., & Offit, P. A. (Eds.). (2013). Vaccines (6th ed.). Saunders.
[6]. Larson, H. J., Jarrett, C., Schulz, W. S., Chaudhuri, M., Zhou, Y., Dube, E., & Wilson, R. (2014). Measuring vaccine hesitancy: The development of a survey tool. Vaccine, 32(34), 4165-4175.
[7]. Clemens, J. D., Jodar, L., & Chokephaibulkit, K. (2015). Use of evidence in WHO recommendations. The Lancet, 385(9978), 563-571.
[8]. Fine, P., Eames, K., & Heymann, D. L. (2011). "Herd immunity": A rough guide. Clinical Infectious Diseases, 52(7), 911-916.
[9]. Larson, H. J., de Figueiredo, A., Xiahong, Z., Schulz, W. S., Verger, P., Johnston, I. G., ... & Dube, E. (2016). The state of vaccine confidence 2016: Global insights through a 67-country survey. EBioMedicine, 12, 295-301.
[10]. Phadke, V. K., Bednarczyk, R. A., Salmon, D. A., & Omer, S. B. (2016). Association between vaccine refusal and vaccine-preventable diseases in the United States: A review of measles and pertussis. JAMA, 315(11), 1149-1158.
[11]. Plans-Rubió, P. (2012). The vaccination coverage required to establish herd immunity against influenza viruses. Preventive Medicine, 55(1), 72-77.
[12]. Dubé, E., Gagnon, D., & MacDonald, N. E. (2015). Strategies intended to address vaccine hesitancy: Review of published reviews. Vaccine, 33(34), 4191-4203.
[13]. Betsch, C., Brewer, N. T., Brocard, P., Davies, P., Gaissmaier, W., Haase, N., ... & Stryk, M. (2012). Opportunities and challenges of Web 2.0 for vaccination decisions. Vaccine, 30(25), 3727-3733.
[14]. Heffernan, J. M., Smith, R. J., Wahl, L. M., & Lipsitch, M. (2005). Understanding the dynamics of rapidly emerging infections: Mathematical models, their assumptions and limitations. Nature Reviews Microbiology, 3(5), 460-468.
[15]. Medley, G. F., & Nokes, D. J. (2006). Evaluating the cost-effectiveness of vaccination strategies: A dynamic perspective. Statistics in Medicine, 25(17), 2936-2948.
[16]. Earn, D. J., & Rohani, P. (1998). Persistence, chaos and synchrony in ecology and epidemiology. Proceedings of the Royal Society of London. Series B: Biological Sciences, 265(1390), 7-10.
[17]. Levin, A., Wang, S. A., Levin, C., & Tsu, V. (2010). Epidemiology of hepatitis B in the Asia-Pacific region. Vaccine, 28(3), 1-7.
[18]. Bloom, D. E., & Canning, D. (2003). Contraception and the Celtic Tiger. Population and Development Review, 29(2), 10-24.
[19]. Rappuoli, R. (2018). Glycoconjugate vaccines: Principles and mechanisms. Clinical Infectious Diseases, 57(7), 1429-1430.
[20]. Akponana, E. B., Egbune, N. J., & Akindele, O. M. (2024). Mathematical modelling of diphtheria transmission dynamics for effective strategies of prevention and control with emphasis on impact of vaccination and waning immunity. International Journal of Research in Engineering and Science, 12(7), 142-153. [https://ijres.org/papers/Volume-12/Issue-7/1207142153.pdf]
[21]. Arierhie, E. O., Egbune, N. J., Akponana, E. B., & Okedoye, A. M. (2024). Strategies and Impacts of COVID-19 Vaccine Rollout: A Deterministic SEIVR Model Approach. International Journal of Research and Scientific Innovation, 11(4), 631-650.
[22]. Akponana, E. B., Arierhie, E. O., Egbune, N. J., & Okedoye, A. M. (2024). Mathematical Modelling of Diphtheria Transmission Dynamics for Effective Strategies of Prevention and Control with Emphasis on Vaccination and Vaccine-Induced Immunity. International Journal of Research in Interdisciplinary Studies, 1(4), 5-14.
[23]. Egbune, N. J., Akponana, E. B., Arierhie, E. O., & Okedoye, A. M. (2024). Mathematical Analysis of Spread and Control of Diphtheria with Emphasis on Diphtheria Antitoxin Efficiency. European Journal of Theoretical and Applied Sciences, 2(3), 152-172.
[24]. Chitnis, N., Hyman, J. M. and Cushing, J. M. "Determining important parameters in the spread of malaria through the sensitivity analysis of a mathematical model," Bulletin of Mathematical Biology, vol. 70, no. 5, pp. 1272–1296, 2008.